Dual-comb electric-field cross-correlation technique for optical arbitrary waveform characterization

Fahmida Ferdous,[1,*] Daniel E. Leaird,[1] Chen-Bin Huang,[2] and A. M. Weiner[1]

[1]*ECE Department, Purdue University, 465 Northwestern Avenue, West Lafayette, Indiana 47907, USA*
[2]*Institute of Photonics Technologies, National Tsing Hua University, Hsinchu, 30013 Taiwan*
**Corresponding author: fferdous@purdue.edu*

Received September 15, 2009; accepted October 21, 2009;
posted November 10, 2009 (Doc. ID 117238); published December 11, 2009

We present an electric-field cross-correlation technique that uses a pair of frequency combs to sweep phase and group delays independently without a mechanical stage. We demonstrate this technique for characterization of optical arbitrary waveforms composed of ~30 spectral lines from a 10 GHz frequency comb. Rapid data acquisition (tens of microseconds) enables interferometric spectral phase measurement of pulses subject to propagation over 20 km of optical fiber. © 2009 Optical Society of America

OCIS codes: 320.5540, 320.7100, 070.7145, 060.0060.

The use of a pulse shaper [1] to manipulate optical frequency combs [2,3] on a line-by-line basis, termed optical arbitrary waveform generation (OAWG) [4–6], leads to new challenges in ultrafast waveform characterization. Waveforms generated through line-by-line pulse shaping exhibit several unique attributes. Such waveforms may exhibit 100% duty cycle, with shaped waveforms spanning the full time-domain repetition period of the frequency comb, and with spectral amplitude and phase changing abruptly from line to line. Although methods for full characterization of ultrashort pulse fields, such as frequency-resolved optical gating and spectral phase interferometry for direct electrical field reconstruction, are well developed [7–9], such methods are typically applied to measurement of low duty-cycle pulses that are isolated in time, with spectra that are smoothly varying, and with relatively low time–bandwidth product. Hence new characterization approaches are desired for shaped waveforms generated from frequency combs. A few techniques for OAWG characterization have recently been reported [6,10–12]. Some of these techniques require a series of measurements performed sequentially, which limits measurement speed [6,10], while others require nonlinear optics and/or an array detector [6,11,12]. Here we demonstrate an electric-field cross-correlation (EFXC) technique in which a precharacterized reference comb is used to measure an unknown signal field from a second optical comb. Although related to standard EFXC techniques, our experiment is constructed in a way uniquely suited to characterization of shaped waveforms from comb sources. Our technique requires only a linear point detector and is simple to construct. It provides both high measurement sensitivity and fast (tens of microseconds) data acquisition.

Our work is closely related to recent coherent multiheterodyne spectroscopy experiments in which a pair of stabilized combs is exploited for rapid measurement of absorption and phase spectra of gas-phase samples [13]. Our work is also related to linear optical sampling [14], which has recently been implemented with dual self-referenced and stabilized ~100 MHz repetition rate comb sources to achieve 15 bit sampling resolution [15]. An important difference is that our setup uses simple comb sources based on modulation of a cw laser [16–18] rather than octave-spanning, self-referenced combs. Furthermore, our simple combs operate at a relatively high repetition rate (10 GHz), which is advantageous both for applications in telecommunications and for arbitrary optical waveform generation, and our measurements are applied to shaped waveform characterization rather than spectroscopy [13].

EFXC measures the interference between a signal field (a_s) and reference field (a_r) in the time domain as a function of the relative delay (τ). Traditionally, the delay is swept using a mechanical translation stage [19]. The resulting time-average power is recorded using a slow photodetector as a function of delay and is written as $\langle P_{\text{out}}(\tau)\rangle = 1/2\{U_s + U_r + \int\{a_s(t)a_r^*(t-\tau)e^{j\omega_0\tau} + \text{c.c.}\}\text{d}t\}$[9]. Here U_s and U_r are the pulse energies and ω_o is the carrier frequency. The unknown signal pulse can be fully recovered from a known, well-characterized reference pulse. Note that in the traditional EFXC scheme, the phase delay and the group delay vary at exactly the same rate. In our scheme the EFXC is recorded without any moving parts. We use two frequency combs with different repetition rates; the difference in the repetition rates (Δf_{rep}) causes the signal and reference pulse envelopes to walk through each other in time $T = 1/\Delta f_{\text{rep}}$. By controlling Δf_{rep}, we can control the group-delay sweep. The phase-delay sweep is controlled by adjusting the offset Δf_{CEO} between the optical center frequencies of the combs (analogous to adjusting the carrier-envelope offset frequency [3]).

Our experimental setup is shown in Fig. 1. A cw laser at 1542 nm is split into reference and signal arms, which are individually modulated to produce ~30 comb lines at 10 GHz line spacing and compressed into approximately bandwidth-limited pulses by using pulse shapers to phase compensate individual frequency components [18]. After phase correction the intensity autocorrelations are in excellent agreement with that simulated assuming flat spectral phase. This provides evidence that our reference

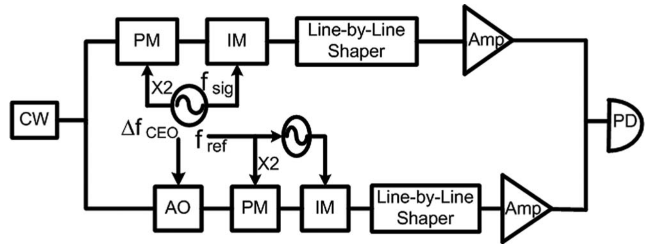

Fig. 1. Schematic of experimental setup. Here Δf_{CEO} is 100 MHz, f_{sig} is 9.953 GHz, f_{ref} is $f_{\mathrm{sig}}+\Delta f_{\mathrm{rep}}$, Δf_{rep} is 220 KHz. CW, continuous-wave laser; PM, phase modulator; IM, intensity modulator; Amp, optical amplifier; PD, photodetector; AO, acousto-optic frequency shifter.

pulse is at least close to transform limited. An acousto-optic modulator is used to provide a $\Delta f_{\mathrm{CEO}}=100$ MHz frequency shift to the signal comb, which sets the EFXC fringe period to 10 ns in time. The comb repetition rates are offset by $\Delta f_{\mathrm{rep}}=220$ kHz, so the group-delay sweeps though the 100 ps comb period in $\sim$4.5 μs. Figure 2(a) shows several periods of the EFXC trace captured using a digital oscilloscope, from which we can easily see the $\sim$4.5 μs periodicity. Figure 2(b) shows a zoom-in view in which we can see the 10 ns fringe period and the 1 ns sampling time. An important point to note is that a full waveform period corresponds to 450 fringes, much fewer than the 20,000 fringes that would be required for a conventional EFXC trace. Our ability to sweep phase and group delay independently significantly reduces the number of fringes that must be recorded, hence easing data-acquisition requirements. Figure 2(a) is EFXC data for an approximately band-limited signal pulse. Here the lack of complete symmetry is attributed to slight differences in both the power spectra and the compensated spectral phase profile of the two combs. An interesting point is that the EFXC from Fig. 2(a) exhibits larger wings than that of the intensity autocorrelation (not shown). Because EFXC depends on field rather than intensity, it is a more sensitive tool to display low amplitude wings. Figures 2(c) and 2(d) show EFXC traces (plotted over 110 ps of equivalent time, slightly more than one waveform period) obtained when the signal-arm line-by-line pulse shaper is programmed to impart respectively an abrupt π phase step and a cubic phase profile onto the spectrum (the specified phase profiles are superimposed onto the phase settings used for compression). Application of a π phase step onto half of the spectrum splits the original pulse into an asymmetric pulse doublet, sometimes termed an odd pulse. The resulting doublet is clearly visible from the EFXC. Cubic spectral phase results in more complicated waveform reshaping with strong oscillatory features. The resulting signal fills the entire waveform period, a clear hallmark of line-by-line pulse shaping.

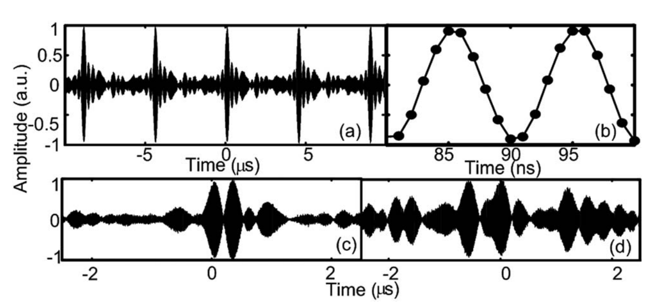

Fig. 2. (a) EFXC data for bandwidth-limited signal showing multiple periods, (b) EFXC data for bandwidth-limited signal zoomed-in to show the fringe period, (c) EFXC data for π-phase step signal, and (d) EFXC data for cubic phase signal.

Spectral information may be retrieved by Fourier analysis of the EFXC data. For conventional EFXC the Fourier transform gives $F\{\langle P_{\mathrm{out}}(\tau)\rangle\}=\ldots+1/2 \times\{A_s(\omega-\omega_o)A_r^*(\omega-\omega_o)+A_s^*(-\omega-\omega_o)A_r(-\omega-\omega_o)\}$, where noninterferometric terms are omitted [9]. In our implementation the first and second terms in this expression appear around $\Delta f_{\mathrm{CEO}}=100$ MHz and -100 MHz, respectively. For our analysis we select the features centered around 100 MHz and set the rest of the Fourier transform to zero. Data consist of a series of discrete lines spaced by $\Delta f_{\mathrm{rep}}=220$ kHz. After we rescale the frequency axis to map the line spacing to the 10 GHz period of our combs, we obtain the spectral amplitude shown in Fig. 3(a). Here we have divided our result by the spectral amplitude profile of the reference, obtained from an optical spectrum analyzer (OSA). The profile in Fig. 3(a) is in qualitative agreement with an independent measurement using an OSA (not shown). The discrete line nature of the retrieved spectrum provides proof that phase coherence is preserved in our EFXC measurements. The average linewidth in Fig. 3(a) is 900 MHz, which corresponds closely to our expectation based on data acquisition over a 50 μs interval (corresponds to 11 waveform periods). Increased linewidths are observed when data are recorded over shorter record lengths, in inverse proportion to the number of waveform periods. We now focus on spectral phase measurements. Figure 3(b) shows spectral phase information obtained for an approximately

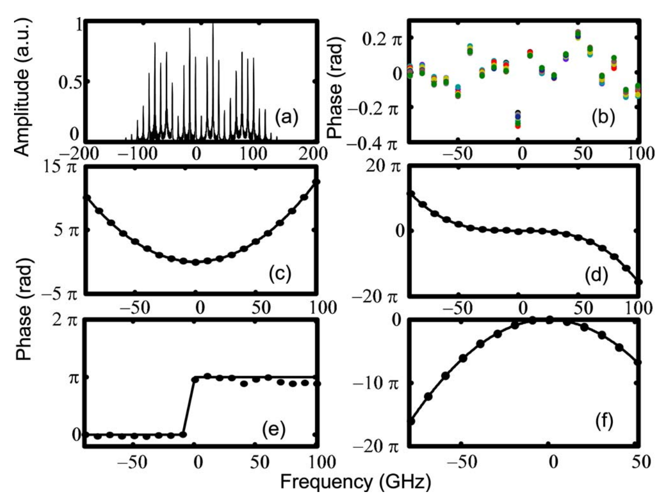

Fig. 3. (Color online) Retrieved (a) amplitude and phase for (b) approximately bandwidth-limited signal, (c) quadratic phase, (d) cubic phase, (e) π-phase step signals obtained via pulse shaper, and (f) after propagation through 20 km optical fiber. In (b) nine sets of data are overlaid. Circles (c)–(f), retrieved phase; lines, applied phase through pulse shaper [(c)–(e)] and quadratic fit (f).

bandwidth-limited signal pulse, with constant and linear spectral phase suppressed. Nine independent data sets are overlaid. The average standard deviation of the results at any one frequency is 0.02π. In contrast, the mean phases show a variation across frequency with 0.1π standard deviation. The latter variation represents errors in the compensated phases of reference and signal fields (more precisely, the difference in the spectral phase errors). Figures 3(c)–3(f) show examples of retrieved phase for shaped signal fields. Here the mean frequency-dependent phases from Fig. 3(b) are subtracted in order to isolate the effect of pulse shaping. Figures 3(c)–3(e) show results obtained when the pulse shaper is programmed (c) for quadratic spectral phase; (d) for cubic spectral phase, EFXC from Fig. 2(d); and (e) for a π phase step, EFXC from Fig. 2(c). In the figures, circles represent retrieved phase values at the peaks of comb lines and lines represent phase functions programmed onto the pulse shaper. Standard deviations between retrieved and programmed phases are $0.5\ \pi$, $0.1\ \pi$, and $0.04\ \pi$ for Figs. 3(c)–3(e), respectively. These results reflect well both on measurement accuracy and pulse-shaping fidelity. Figure 3(f) shows spectral phase retrieved after the signal field is transmitted through 20 km of standard single-mode fiber. For this measurement Δf_{rep} was increased to 850 kHz. The standard deviation between the retrieved phase and a quadratic fit (solid line) is 0.1π. The dispersion coefficient is calculated as 16.5 ps/(nm-km), consistent with the known dispersion of the standard single-mode fiber. This result demonstrates the ability to perform EFXC over a significant length of fiber, with accuracy comparable to that obtained in experiments without long fibers and on a time scale fast enough that fiber fluctuations do not significantly degrade the interferometric measurement process.

In summary, we have demonstrated a simple electric-field cross-correlation technique that exploits the properties of frequency combs for rapid characterization of optical arbitrary waveforms. Spectral phase measurement of pulses dispersed by propagation over 20 km of optical fiber is also presented.

This work was supported by the Defense Adavanced Research Project Agency (DARPA)/Army Research Office (USARO) under grant W911NF-07-1-0625 as part of the DARPA Optical Arbitrary Waveform Generation (OAWG) program and by the National Science Foundation (NSF) under grant ECCS-0601692. Helpful discussions with V. R. Supradeepa are gratefully acknowledged.

References

1. A. M. Weiner, Rev. Sci. Instrum. **71**, 1929 (2000).
2. Th. Udem, R. Holzwarth, and T. W. Hänsch, Nature **416**, 233 (2002).
3. D. J. Jones, S. A. Diddams, J. K. Ranka, A. Stentz, R. S. Windeler, J. L. Hall, and S. Cundiff, Science **288**, 635 (2000).
4. Z. Jiang, D. S. Seo, D. E. Leaird, and A. M. Weiner, Opt. Lett. **30**, 1557 (2005).
5. Z. Jiang, C.-B. Huang, D. E. Leaird, and A. M. Weiner, Nat. Photonics **1**, 463 (2007).
6. R. P. Scott, N. K. Fontaine, J. Chao, K. Okamoto, B. H. Kolner, J. P. Heritage, and S. J. B. Yoo, Opt. Express **15**, 9977 (2007).
7. D. J. Kane and R. Trebino, IEEE J. Quantum Electron. **29**, 571 (1993).
8. C. Iaconis and I. A. Walmsley, Opt. Lett. **23**, 792 (1998).
9. A. M. Weiner, *Ultrafast Optics* (Wiley, 2009).
10. Z. Jiang, D. E. Leaird, and A. M. Weiner, J. Lightwave Technol. **24**, 2487 (2006).
11. V. R. Supradeepa, D. E. Leaird, and A. M. Weiner, Opt. Express **17**, 25 (2009).
12. H. Miao, D. E. Leaird, C. Langrock, M. M. Fejer, and A. M. Weiner, Opt. Express **17**, 3381 (2009).
13. I. Coddington, W. C. Swann, and N. R. Newbury, Phys. Rev. Lett. **100**, 013902 (2008).
14. C. Dorrer, D. C. Kilper, H. R. Stuart, G. Raybon, and M. G. Raymer, IEEE Photon. Technol. Lett. **15**, 1746 (2003).
15. I. Coddington,W. C. Swann, and N. R. Newbury, Opt. Lett. **34**, 2154 (2009).
16. H. Murata, A. Morimoto, T. Kobayashi, and S. Yamamoto, IEEE J. Sel. Top. Quantum Electron. **6**, 132 (2000).
17. T. Sakamoto, T. Kawanishi, and M. Izutsu, Opt. Lett. **32**, 1515 (2007).
18. C. B. Huang, S. G. Park, D. E. Leaird, and A. M. Weiner, Opt. Express **16**, 2520 (2008).
19. K. Naganuma, K. Mogi, and H. Yamada, Opt. Lett. **15**, 393 (1990).